

Dust Opacities inside Dust Devil Column in the Taklimakan Desert

Zhaopeng Luan^{1,2,3}, Yongxiang Han^{1,2}, Tianliang Zhao^{1,2}, Feng Liu^{1,2}, Chong Liu^{1,2},

Mark J. Rood⁴, Xinghua Yang⁵, Qing He⁵, Huichao Lu³

¹ Collaborative Innovation Center on Forecast and Evaluation of Meteorological Disasters,
Nanjing University of Information Science and Technology, Nanjing, 210044, China

² Key Laboratory for Aerosol-Cloud-Precipitation of China Meteorological Administration,
Nanjing University of Information Science and Technology, Nanjing, 210044, China

³ Tai'an Meteorological Bureau, Tai'an, 271000, China

⁴ Department of Civil & Environmental Engineering, University of Illinois at Urbana-Champaign,
Illinois, 61820, USA

⁵ Institute of Desert Meteorology, China Meteorological Administration, Urumqi, 830002, China

Correspondence to: Tianliang Zhao (tlzhao@nuist.edu.cn)

Abstract. The distribution of dust aerosols in dust devils (DDs) is quantitatively characterized here based on a field observation. We applied the Digital Optical Method (DOM) with digital still cameras to quantify the opacity of the DDs in the Taklimakan Desert, China. This study presents the following unique and important results: 1) the distinct horizontal distributions of opacity proved the existence of DDs' eye, similarly to the eye of tropical cyclone; 2) The opacity of the DDs decreases with increasing height, however, the dust aerosols do appear to settle out, and the relatively calm eye leads to a minimum in dust opacity at the eye; 3) The horizontal distribution of opacity is quasi symmetric with a bimodal across the eye of the DDs, which could be resulted from the ambient air conditions; and 4) A new method is developed for

1 characterizing the three-dimensional structure of DDs based on the observed
2 two-dimensional opacity provided by DOM. This study not only proposes a highly
3 reliable, low cost and efficient methodology to capture the optical structure of DDs,
4 but also could provide the information on estimation of dust emissions driven by DDs.

5 **Keywords:** dust devil; digital optical; opacity; dust devil eye; 3-D structure

6

7 **1 Introduction**

8 Well-defined vortexes that range from 1 m to 1,000 m tall (Lorenz et al., 2016),
9 also known as dust devils (DDs) are the most common small scale (< 50 m diameter
10 at ground level) dust transmitting system in the atmosphere(Lorenz et al., 2016;
11 Kanak, 2005;Kanak et al., 2000;Leovy, 2003). It is a special case of columnar,
12 ground-based convective vortex occurring in the lower atmospheric boundary
13 layer(Gu et al., 2008;Koch and Renno, 2005). Occurrences of wind devils are
14 associated with weak wind and sunny weather. As the near surface air temperature
15 rises with the increase of surface sensible heat under heterogeneous solar radiation,
16 the thermal convection is driven by the thermal buoyancy in the convective boundary
17 layer, consequently leading to vortex rotation containing particulate matters with large
18 angular momentums (Kanak, 2005; Klose et al., 2016). And the radius of wind devil is
19 mainly determined by the initial angular momentum of the air mass(Gu et al., 2010).
20 DDs have significant potential for high dust loadings, contributing to one third of the
21 total natural particulate mass emitted to the atmosphere annually (Koch and Renno,
22 2005). Emissions of total primary particulate mass by DDs to the atmosphere are as

1 high as 65% in the United States (Gillette and Sinclair, 1990). About 77%-87% of the
2 primary particulate mass emitted to the atmosphere in Chinese deserts is caused by
3 DDs(Han et al., 2008;Deng et al., 2011;Zhang et al., 1994), while recent study show
4 that global dust uplift by DDs is about 3.4%(Jemmett-Smith et al., 2015) even 1%
5 (Klose et al., 2016; Metzger et al.,2011). But some key factors like dust flux per DD
6 and the fractional updraft area occupied by DDs in a convectively active region are
7 still uncertainty in the calculation. Dust particles are more easily released from the
8 surface by DDs through the “ ΔP -effect” of pressure fluctuations (Greeley et al., 2003;
9 Neakrase et al., 2016). And particle lifting processes depend on structure and
10 morphology of DDs, internal meteorological characteristics like internal pressure
11 structure, and ambient conditions (Neakrase et al.,2016). However, physical processes
12 and mechanisms of dust entrainment by DDs are poorly understood. It is extremely
13 difficult to observe DDs because of their sporadic and unpredictable mobile paths. So
14 the basic structure and characteristic parameters have long been based on human
15 observations by Ives (1947)and Sinclair (1964). DDs’ central core structure has been
16 remarkably observed with mobile Doppler radar (Bluestein et al., 2004) and their
17 center pressure has been characterized by pressure logger (Lorenz, 2012;Lorenz,
18 2013). In addition, LES (Large Eddy Simulation) have also been applied to DD
19 studies by Toigo (2003) and Ito et al.(2010). The condition of weaker wind and
20 stronger surface heat flux favorable for the formation of dust devil is confirmed
21 according to theirs studies. Gu et al. (2003; 2010) provided the meteorological
22 characteristics inside of DDs by numerical simulation. And Klose and Shao (2016)

1 simulated DD by using WRF/LES-Dto, revealing that the maximum emissions are
2 determined by atmospheric stability. However, field observations of DDs for
3 validating the modeling results including vortex dynamics are critical and necessary
4 (Leovy, 2003).

5 The Digital Optical Method (DOM) was developed to measure opacities of plumes
6 emitted from stationary point sources (Du et al., 2007; Du et al., 2009). DOM uses a
7 digital still camera and software for processing the digital pictures to determine plume
8 opacity. This method was also used to quantify plume opacities for fugitive dust
9 plumes (Du et al., 2013). DOM was developed to provide digital record of plume
10 opacity at low cost, easy implementation, with improved accuracy compared to human
11 observations of plume opacity.

12 We conducted a DD field campaign in the Taklimakan Desert, the largest desert in
13 China and the world's second largest liquidity desert during July 2014. This study is
14 the first to apply DOM to characterize the internal structure of DDs in the Taklimakan
15 Desert. Two dimensional (2D) structures of dust devils are archived with the digital
16 images of the DD by processing with DOM software. This effort provides horizontal
17 and vertical distributions of opacity values in DDs, and presents the three-dimensional
18 (3D) opacity structure of DDs. It is important to quantify the structure of DDs. The
19 study thus services to provide insightful information for DD formation mechanism
20 and numerical simulation.

21

22 **2 Methods**

2.1 Image acquisition and processing

The observational site is located in the Xiaotang region ($40^{\circ}50'N$, $84^{\circ}10'E$, altitude 943.9m), in the hinterland of the Taklimakan Desert (see Fig.1). Xiaotang is a typical desert-Gobi transitional zone where DDs occur frequently according to local meteorological observations. During the observations from 2 to 14 July, 2014, digital images were captured with two digital still cameras (Sony Cyber-shot Model DSC-P100). In order to obtain the appropriate background for taking the pictures, the camera is back to the sun within a 140° sector (ASTM D-7520). All the pictures archived as JPEG files. Most observed DDs show inverted circular cone in the quasi-symmetric shape across the DD's eye with a height of several tens to hundreds meters. None of the DDs have absolute symmetry caused by the time-dependent dynamics.

A digital image of a typical DD is illustrated in Fig.1 to describe how to determine the DD opacity values. The vertical curved lines were added to the image to represent auxiliary lines describing vertical grids for estimation of opacity values. The sky background of the DD is relatively uniform as shown in Fig.1. 15 large dust devils were observed during the observation period. And this case was selected with a reference substance for the DD's scale. The upright electric pole right next to the DD with a height of 4.5 m was a reference to measure the height and diameter of the DDs. The DD with a base radius of 6.4 m and a height of 23.0 m has a maximum diameter of 15.8 m at the height of 16.0 m. We defined the "upper end" of a dust devil with the opacity of near to zero. In order to examine the spatial distribution of dust aerosols

within the DD's dust cone, we horizontally set the cone into 0.4 m grids with 15 auxiliary upward lines parallel to the DD's conical surface. The centerline (line 0) is a vertical line from the bottom of the DD's eye. For the further analysis of DD structure, we count lines on the left of the centerline from 1 to 7, while denoting lines to the right of the center from A to H (Fig.1b).

2.2 Calculation of opacity

DOM's transmission model was used in this study due to the uniform background sky conditions (e.g., uniform clear or overcast sky) for the DDs. And the challenge to install contrasting backgrounds behind and next to the DDs as needed with DOM's contrast model (Du et al., 2007). The transmission model calculates the plume's opacity based on the radiance from the plume and the radiance from the plume's background. Part of the radiance (N_0) from the sky is lost as it passes through the plume due to light scattering and/or absorption. N denotes the radiances received by the charge-coupled device (CCD) of the digital camera that correspond to the sky background, in terms of pixel values:

$$N = N_0 T_0 + N^*$$

T_0 denotes the transmittance of the plume-free atmosphere along the path between the camera and the sky background. N^* is the path radiance of the atmosphere along the same path, which is from direct, diffuse, and reflected radiances scattered into the sight path by ambient air and aerosols (Du et al., 2013), and can be estimated with an equilibrium radiance model for uniform illumination and negligible absorption:

$$N^* = N_0(1 - T_0)$$

From the two equation, getting the results of $N=N_0$.

Therefore, when the radiance reaches the camera (N_p), it is caused by the attenuated radiance value from the plume (N_{T1}), diffusive radiance value (N_{T2}), and attenuation of the radiance caused by the surrounding atmosphere (which is negligible compared to the DD). The attenuated radiance value (N_{T1}) results from N_0 after the light is scattered and/or absorbed by the plume and the diffusive radiance value (N_{T2}) is caused by other sources of light than the uniform sky background (Fig.2). According to the definition of opacity:

$$Opacity = 1 - \frac{N_{t1}}{N_0} = 1 - \frac{N_p - N_{t2}}{N}$$

Because the camera did not directly measure N_{t2} , the proportionality coefficient, K , is defined by $N_{t2}=K*N*Opacity$ (Du et al., 2007), and then the plume opacity could be determined by the transmission model as described by:

$$Opacity = \frac{1 - \frac{N_p}{N}}{1 - K}$$

N_p is the equivalent radiance value recorded by the camera, in terms of pixel values, caused by radiance from the plume (N_T) and path radiance of the atmosphere. N is the equivalent radiance value recorded by the camera, in terms of pixel values, after N_0 passes through the DD-free atmosphere. K value of 1.4 in the transmission model is used.

3 Results and analysis

3.1 The vertical profile of opacity

Fig.3a and Fig.3b demonstrate the opacity profiles of the vertical lines, as shown in

Fig.1. It can be seen that: 1) The opacity profiles are non-uniform in the vertical direction, and the vertical variation of opacity becomes more significant from the inner to the outer portions of the conical dust plume (See from the both Fig.3a and Fig.3b), 2) The opacity profiles from center to both sides show only a quasi-symmetry; and 3) The opacity values generally decrease with height with the larger change rates at lower levels than upper ones. The averaged lapse rates (percent change in opacity values with increasing height) for the profile are 4.1% and 0.6% per meter respectively below and over the height of 10 m.

3.2 The horizontal variation of opacity

From the horizontal variation of the opacity at different levels (Fig.4), it is observed that: 1) the horizontal opacity values increase first and then decrease from the center part to both sides at the base of the DD; 2) The opacity within the DD are decreasing with height with a monotonically decreasing function. The maximum opacity is observed at the bottom of the DD; and 3) on the right side of the DD, the magnitude of opacity is greater than the left side. The DOM method is able to capture all important well-known natures of DD including non-absolute symmetry and internal inhomogeneity.

3.3 Two-dimensional distribution of the quantized DD's opacity

The 2D distribution of the DDs reflects the basic features of inhomogeneity and quasi-symmetry inside the DD. The method to quantify spatial distribution of opacity is able to present the similar spatial variability like grid boxes defined in DD numerical models to simulate spatial distribution of physical properties(Mason et al.,

2013;Gu et al., 2006).In addition, other cases with the undermined height and width of DDs also show the similar structures(Fig.5).

The opacity is related to the aerosol concentration, composition, and size distribution in DDs (Metzger et al., 1999). The value of the opacity is assumed to decrease with increasing height due to gravity that prevents larger particles from traveling to the upper parts of the DD. Therefore, it is expected that smaller particles could be transmitted to a higher altitudes(Gu et al., 2003;Gu et al., 2007). A distinct vertical opacity gradient develops with small values at the center portion of the DD. The large particles decrease due to the gravitational settling and the fine particles continue to rise with height. However, the change of vertical air flow could lead to the vertical decreases in concentrations of fine dust for the declining opacity of DDs with height. These results are consistent with those from numerical simulations by Gu (2007) and Gierasch (1973; 1974).

3.4 The DD eye and the three dimensional distribution of opacity

Previous research have clarified the principal characteristics of DDs with the centers of low pressure, weak airflow, and almost zero tangential velocity (Fiedler and Kanak, 2001;Kanak, 2006). Dust concentrations in this inner core region are much lower compared to other portion of DD (Balme and Greeley, 2006;Gu et al., 2003). It is similar to the eye of hurricanes or typhoons characterized with light wind, clear skies. Though the DD's eye is difficult to observe directly, the variation of opacity with a bimodal distribution at the same height (Fig.4) confirms the existence of DD's eye. Fig.6 illustrates a conceptual mode of the horizontal cross section of a DD. The

1 DD's eye diameters are measured by $2R$ and $2r$, respectively, The line segment FG is
2 the distance between two peak opacity points F and G, H with minimum opacity is the
3 center of the eye. The opacity value at point A in Fig.6, for instance, is the
4 accumulated opacity through distance from B to C. We assumes the horizontal opacity
5 values are constant between B and C.

6 A more detailed example in Fig.4 describes the DD with the diameter of 12 m and
7 the height of 4 m. The horizontal variation of opacity shows an obvious bimodal
8 distribution. The peak opacity value is located at 3 m away from the DD's centerline.
9 Therefore, it can be determined that the outer radius of DD is 6 m and the inner radius
10 of DD's eye is 3 m at the same height. Every segment (e.g., B to C) is divided into
11 four equal sub-segments, and the horizontal distribution can be derived accordingly.
12 By calculating the horizontal distribution at different heights (i.e., at 3m, 6 m, 9 m,
13 and 12 m), we present the 3D structure of DD as shown in Fig.7. The opacity values
14 increase first and then decreases from the center to both sides of the DD for the
15 bimodal distribution. The 3D structure of DD in Fig.7 represents the inhomogeneity
16 and quasi-symmetric opacity distribution.

17 The results demonstrate that themethodology to derive the 3D structure in a DD is
18 feasible and practicable. The future effort to improve this methodology is to identify
19 and quantify discrepancies between the assumed and observed opacity values from B
20 to C. It can be realized using more cameras to capture digital images of the same DD
21 from different angles. The more precise 3D structure of DD could be built with the
22 improved measurements.

1

2 **4 Conclusions and discussions**

3 This study applied Digital Optical Method (DOM) to quantify the opacity of dust
4 devils (DDs) in the Taklimakan Desert. The two dimensional (2D) distribution of
5 opacity inside the DD was obtained by DOM. Analysis results show that the opacity
6 values of DDs decrease monotonically with height with the averaged lapse rate of 4.1%
7 and 0.6% below and over 10 m height. The opacity values from the DD's eye to both
8 edges of the DD horizontally increases, reaches a peak value, and then diminishes
9 rapidly, charactering the quasi-asymmetry of dust particles inside DDs by the bimodal
10 distribution. The distinct horizontal distribution of opacity values confirms the
11 existence of the DD's eye. A typical 3D structure of opacities is built based on the
12 assumption of constant opacity through horizontal cross-sections of a DD.

13 In order to improve the quality of DD observations using DOM, the following key
14 issues will be addressed: 1) the proportionality coefficient (K) is not available so far
15 for desert dust devils. The K value we used in our opacity calculations is for white
16 plume (light scattering plume) whose optical properties is definitely different from
17 DD (desert dust particles), the value of K for desert dust is identified as a urgent need
18 for our future study; 2) a scaling model of DD size is required if there is no references
19 for DD scale; 3) the results documented in this study are far from generalized
20 characteristics of DD opacity. In order to realize statistical analysis of large sized
21 samples, more observations including carefully-designed specific field campaigns are
22 needed for characterizing DD opacities; 4) the validation of calculated opacities inside

1 DD column is also a challenge. It is essential to collect other independent observation
2 data of DD for this purpose.

3 In this study, the lines are chosen to follow a conical pattern rather than a regular
4 grid, just for the simple characterization of the optical structure of DDs. The method
5 to quantify spatial distribution of opacity is able to present the similar spatial
6 variability like grid boxes defined in DD numerical models to simulate spatial
7 distribution of physical properties (Mason et al., 2013; Gu et al., 2006). In the further
8 study, we could use the regular grids for a better comparison between differently
9 shaped dust devils, in particular for dust devils that are not well-structured and might
10 deviate substantially from an ideal conical shape.

11 A new method to convert 2D structure of opacity using multiple-camera digital
12 optical method (MDOM) to 3D will be developed for the better estimation of vertical
13 gradient of dust concentrations. In addition, the wind shear and Reynolds stress will be
14 considered in the improved system in order to realize the parameterization of vertical
15 dust flux caused by DDs.

16 The opacity of dust devils may also be affected by meteorology like ambient wind
17 and temperature difference between surface and air (Liu et al. 2016), which could
18 influence the structures of dust devils. High-strength dust devils can roll up more dust
19 particles, affecting the opacity of dust devils. So in the further study, more
20 comprehensive observations will be set to measure meteorology such as ambient wind,
21 heat exchanges between surface and air, wind of dust devils, temperature and pressure
22 difference between core of dust devils and surrounding environment, etc.

1

2 **Acknowledgments**

3 This research was supported the National Natural Science Foundation of
4 China(41375158;41175093;41405013) and the Research Starting Project of NUIST
5 (20110304) of China. Any opinions, findings, and conclusions or recommendations
6 expressed in this paper are those of the authors and do not necessarily reflect the view
7 of the Nanjing University of Information Science and Technology, University of
8 Illinois at Urban and Champaign, or any organizations and government agencies.

9

10 **References**

- 11 American Society of Testing Materials Standard Test Method for Determining the
12 Opacity of a Plume in the Outdoor Ambient Atmosphere (ASTM D-7520),
13 <http://www.astm.org/Standards/D7520.htm>, 2013.
- 14 Balme, M., and Greeley, R.: Dust devils on Earth and Mars, Reviews of Geophysics,
15 44, doi: 10.1029/2005RG000188, 2006.
- 16 Bluestein, H. B., Weiss, C. C., and Pazmany, A. L.: Doppler radar observations of
17 dust devils in Texas, Monthly weather review, 132, 209-224, doi: [http://dx.doi.org/10.1175/1520-0493\(2004\)132<0209:DROODD>2.0.CO;2](http://dx.doi.org/10.1175/1520-0493(2004)132<0209:DROODD>2.0.CO;2), 2004.
- 18 Deng, Z.Q., Han, Y.X., Bai, Z.H.,and Zhao, T.L.:Relationship between dust aerosol
19 and solar radiation in gebi desert in North China.China Environment Science,
20 31(11):1761-1767,2011.(In Chinese)
- 21 Du, K., Rood, M. J., Kim, B. J., Kemme, M. R., Franek, B., and Mattison, K.:
22 Quantification of plume opacity by digital photography, Environmental science &
23 technology, 41, 928-935, doi: 10.1021/es061277n, 2007.
- 24 Du K., Rood, M. J., Kim, B.J., Kemme, M. R., Franek, B., and Mattison, K.:
25 Evaluation of digital optical method to determine plume opacity during nighttime.
26

1 Environmental science & technology, 43, 783-789, doi: 10.1021/es800483x, 2009.

2 Du, K., Shi, P., Rood, M. J., Wang, K., Wang, Y., and Varma, R. M.: Digital Optical
3 Method to quantify the visual opacity of fugitive plumes, Atmospheric Environment,
4 77, 983-989, doi:10.1016/j.atmosenv.2013.06.017, 2013.

5 Fiedler, B. H., and Kanak, K. M.: Rayleigh- Bénard convection as a tool for studying
6 dust devils, Atmospheric Science Letters, 2, 104-113, doi : 10.1006/asle.2001.0046,
7 2001.

8 Gillette, D. A., and Sinclair, P. C.: Estimation of suspension of alkaline material by
9 dust devils in the United States, Atmospheric Environment. Part A. General Topics,
10 24, 1135-1142, doi:10.1016/0960-1686(90)90078-2,1990.

11 Greeley R., M.R. Balme, J.D. Iversen, S. Metzger, R. Mickelson, J. Phoreman, B.
12 White: Martiandust devils: laboratory simulations of particle threshold. J. Geophys.
13 Res. 108, 5041, doi:10.1029/2002JE001987, 2003.

14 Gu, Z., Zhao, Y., Yu, Y., and Feng, X.: Numerical study of the formation evolution
15 and structure of dust devil. Acta Meteorologica Sinica, 61, 751-760,2003.(In Chinese)

16 Gu, Z.L., Wei, W., and Zhao, Y.Z.: An overview of surface conditions in numerical
17 simulations of dust devils and the consequent near-surface air flow fields. Aerosol Air
18 Qual. Res, 10, 272-281, doi: 10.4209/aaqr.2009.12.0077, 2010.

19 Gu, Z. L., Qiu, J., Lu, L.Y., and Zhao,Y.Z.: Advances in Study of Dust Devils,
20 Journal of Desert Research, 5, 022, 2007. (In Chinese)

21 Gu, Z., Zhao, Y., Li, Y., Yu, Y., and Feng, X.: Numerical simulation of dust lifting
22 within dust devils-simulation of an intense vortex, Journal of the atmospheric sciences,
23 63, 2630-2641, doi: http://dx.doi.org/10.1175/JAS3748.1, 2006.

24 Gu, Z., Qiu, J., Zhao, Y., and Hou, X.: Analysis on dust devil containing loess dusts
25 of different sizes, Aerosol Air Qual. Res, 8, 65-77, doi:10.4209/aaqr.2007.03.0026,
26 2008.

27 Gierasch, P., and Goody, R.: A model of a Martian great dust storm. Journal of the
28 AtmosphericSciences,30,169-179,doi: http://dx.doi.org/10.1175/1520-0469(1973)030
29 <0169:AMOAMG>2.0.CO;2,1973.

30 Gierasch, P. J.: Martian dust storms. Reviews of Geophysics, 12, 730-734,

1 doi: 10.1029/RG012i004p00730,1974.

2 Han, Y., Fang, X., Xi, X., Song, L., and Yang, S.: Dust storm in Asia continent and its
3 bio-environmental effects in the North Pacific: A case study of the strongest dust
4 event in April, 2001 in central Asia, Chinese Science Bulletin, 51, 723-730,
5 doi:10.1007/s11434-006-0723-2, 2006.

6 Han, Y., Dai, X., Fang, X., Chen, Y., and Kang, F.: Dust aerosols: a possible
7 accelerant for an increasingly arid climate in North China, Journal of Arid
8 Environments, 72, 1476-1489,2008,doi:10.1016/j.jaridenv.2008.02.017, 2008.

9 Ives, R. L.: Behavior of dust devils. Bull. Amer. Meteor. Soc, 28, 168-174,1947.

10 Ito, J., Tanaka, R. and Niino, H.: Large eddy simulation of dust devils in a
11 diurnally-evolving convective mixed layer. Journal of the Meteorological Society of
12 Japan, 88,63-77, doi:10.2151/jmsj.2010-105, 2010.

13 Jemmett - Smith B C, J H Marsham, P Knippertz, and C A Gilkeson:Quantifying
14 global dust devil occurrence from meteorological analyses. Geophysical Research
15 Letters, 42, 1275-1282, doi:10.1002/2015GL063078, 2015.

16 Klose M. and Y. P. Shao: A numerical study on dust devils with implications to
17 global dust budget estimates. Aeolian Research,22, 47-58,doi:
18 http://dx.doi.org/10.1016/j.aeolia.2016.05.003, 2016.

19 Kanak, K. M., Lilly, D. K., and Snow, J. T.: The formation of vertical vortices in the
20 convective boundary layer, Quarterly Journal of the Royal Meteorological Society,
21 126, 2789-2810, doi: 10.1002/qj.49712656910, 2000.

22 Kanak, K. M.: Numerical simulation of dust devil-scale vortices, Quarterly Journal of
23 the Royal Meteorological Society, 131, 1271-1292, doi: 10.1256/qj.03.172, 2005.

24 Kanak, K. M.: On the numerical simulation of dust devil-like vortices in terrestrial
25 and Martian convective boundary layers, Geophysical research letters, 33,
26 doi: 10.1029/2006GL026207, 2006.

27 Koch, J., and Renno, N. O.: The role of convective plumes and vortices on the global
28 aerosol budget, Geophysical research letters, 32, doi: 10.1029/2005GL023420, 2005.

1 Leovy, C. B.: Mars: The devil is in the dust, *Nature*, 424, 1008-1009,
2 doi:10.1038/4241008a, 2003.

3 Lorenz R.D., M. R. Balme, Z. L. Gu, H. Kahanpaa, M. Klose, M. Kurgansky, M. R.
4 Patel, D. Reiss, A. P. Rossi, A. Spiga, T. Takemi, W. Wei: History and Applications
5 of Dust Devil Studies. *Space Sci Rev*, 203,5-37,doi:10.1007/s11214-016-0239-2,
6 2016.

7 Lorenz, R.: Observing desert dust devils with a pressure logger, *Geoscientific*
8 *Instrumentation, Methods and Data Systems*, 1, 209-220, doi:10.5194/gi-1-209-2012,
9 2012.

10 Lorenz, R. D.: Irregular dust devil pressure drops on Earth and Mars: Effect of
11 cycloidal tracks, *Planetary and Space Science*, 76, 96-103,
12 doi:10.1016/j.pss.2013.01.001, 2013.

13 Liu, C., T. Zhao, X. Yang, F. Liu, Y. Han, Z. Luan, Q. He, M. Rood, and W. Yuen:
14 Observational study of formation mechanism, vertical structure, and dust emission of
15 dust devils over the Taklimakan Desert, China, *J. Geophys. Res. Atmos.*, 121,
16 3608–3618, doi:10.1002/2015JD024256, 2016.

17 Marsham, J., Parker, D., Grams, C., Johnson, B., Grey, W., and Ross, A.:
18 Observations of mesoscale and boundary-layer scale circulations affecting dust
19 transport and uplift over the Sahara, *Atmospheric Chemistry and Physics*, 8,
20 6979-6993, doi:10.5194/acp-8-6979-2008, 2008.

21 Metzger S. M., M.R. Balme, M.C. Towner, B.J. Bos, T.J. Ringrose, M.R. Patel: In
22 situ measurements of particle load and transport in dust devils. *Icarus*, 214, 766–772,
23 doi:10.1016/j.icarus.2011.03.013, 2011.

24 Mason, J. P., Patel, M. R., and Lewis, S. R.: Radiative transfer modelling of dust
25 devils, *Icarus*, 223, 1-10, doi:10.1016/j.icarus.2012.11.018, 2013.

26 Metzger, S. M., Carr, J. R., Johnson, J. R., Parker, T. J., and Lemmon, M. T.: Dust devil
27 vortices seen by the Mars Pathfinder camera. *Geophysical research letters*, 26,

1 2781-2784, doi: 10.1029/1999GL008341,1999.

2 Neakrase L.D.V., M.R.Balme, F.Esposito, T. Kelling, M. Klose, J.F. Kok, B.

3 Marticorena, J. Merrison, M. Patel, G. Wurm: Particle Lifting Processes in Dust

4 Devils.Space Sci Rev,203,347–376, doi: 10.1007/s11214-016-0296-6, 2016.

5 Sinclair, P. C.: Some preliminary dust devil measurements. Monthly Weather Review,

6 92,doi:http://citeseerx.ist.psu.edu/viewdoc/download?doi=10.1.1.395.3338&rep=rep1

7 & type=pdf, 1964.

8 Toigo, A. D., M. I. Richardson, S. P. Ewald, and P. J. Gierasch: Numerical simulation

9 of Martian dust devils. Journal of Geophysical Research: Planets (1991–2012), 108,

10 doi: 10.1029/2002JE002002, 2003.

11 Wei L. and Shen,Z.B.:The radiative characteristics of atmospheric dust observed from

12 satellite.J.Plateau Meteorology,17(4):347-355,1998.(In Chinese)

13 Wang, M., and Zhang, R.: Frontier of atmospheric aerosols researches, Climatic and

14 Environmental Research, 6, 119-124, 2001.(In Chinese)

15 Zhang X.Y.,An, Z.S., Zhang, G.Y., Chen, T., Liu, D.S., Arimoto, R.:Transport,

16 deposition and reflected climate change of Chinese atmospheric particulate-I. Modern

17 Atmospheric Aerosols, J. Science in China, 24(12):1314-1322,1994. (In Chinese)

18

19

20

21

22

23



Fig.1. A typical DD observed on July 2, 2014 with (a) the original photo and (b) the image marked with black lines, letters and numbers for the analysis of DD vertical structures. An upright pole near the DD as a reference for measuring the DD)

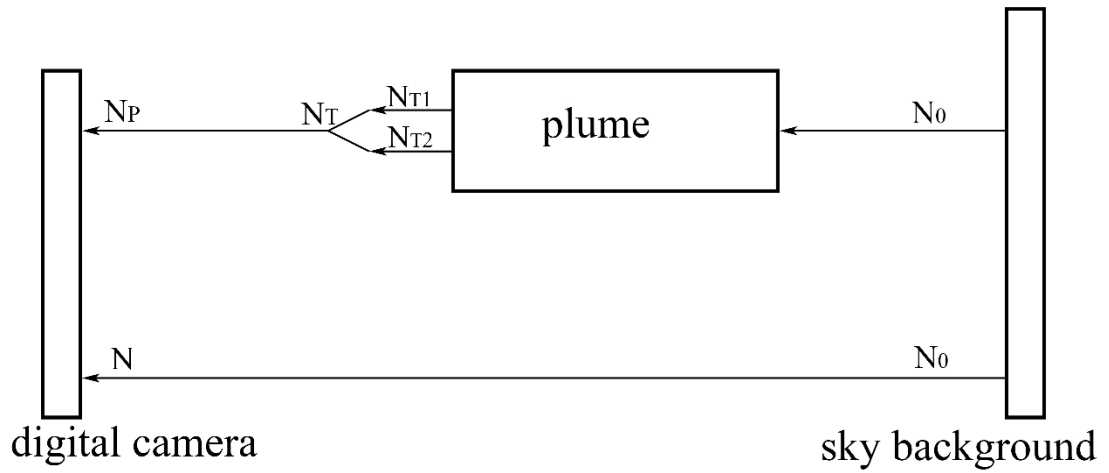


Fig.2. Schematic of the transmission model determining plume opacity

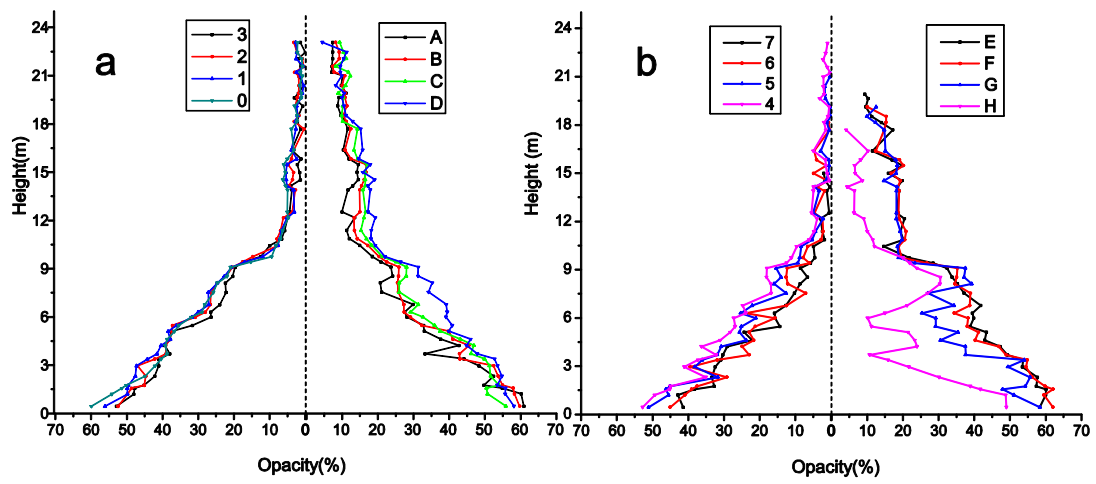


Fig.3.Vertical opacity profiles of dust devils

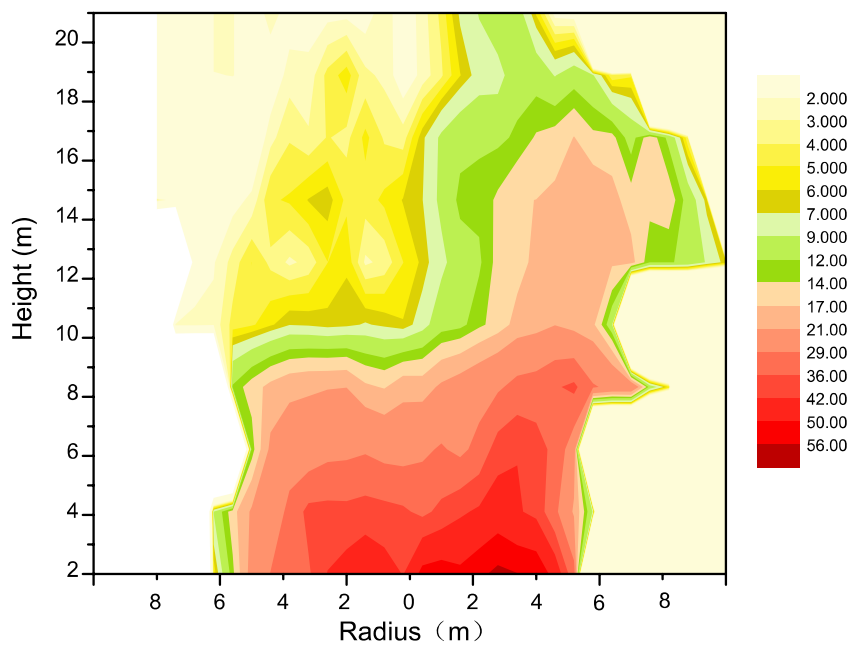


Fig.4.Horizontal variation of the DD's opacity(%) at different levels

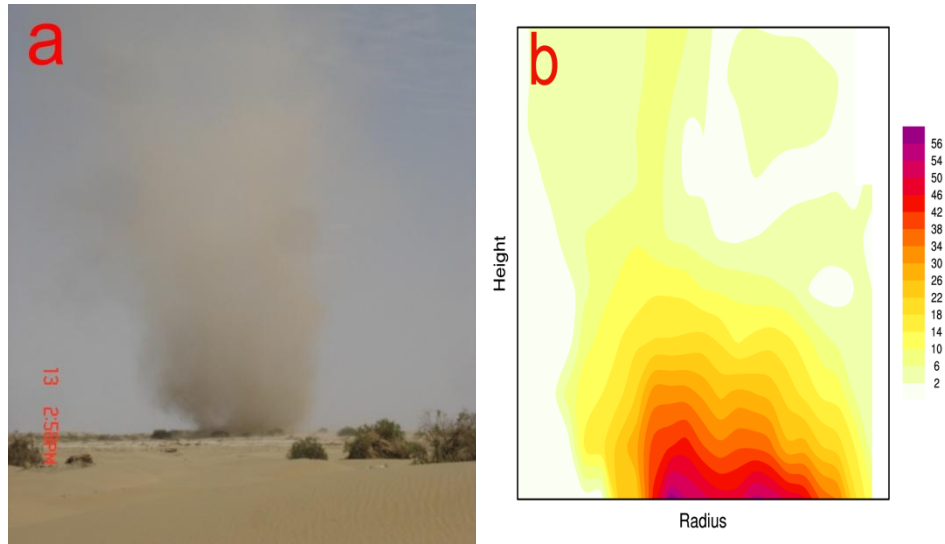


Fig.5. The DD observed on July 13, 2014 with (a) original photo and (b) the quantized DD's opacity

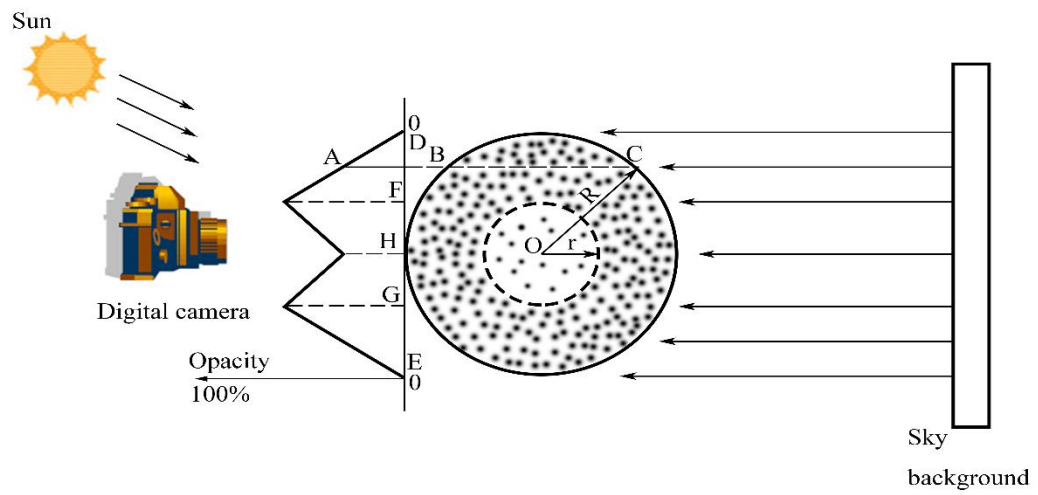


Fig.6.A diagram of DD's horizontal section model with variation of opacity

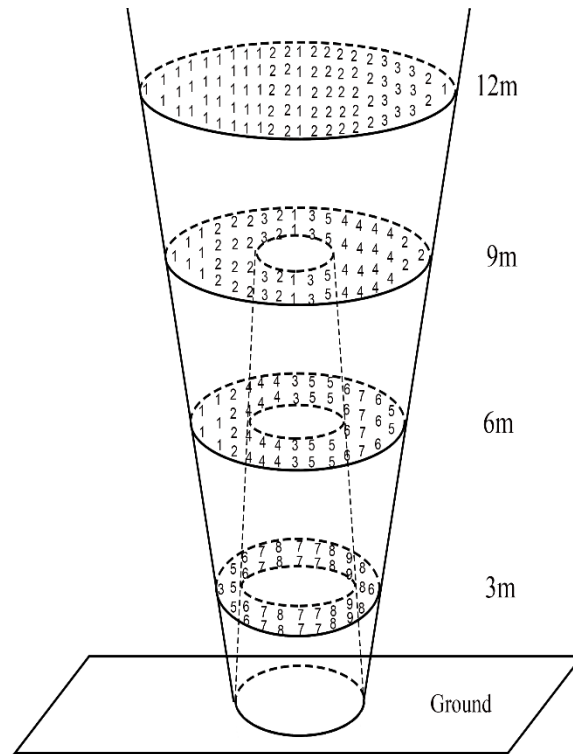


Fig.7. A 3D structure of the DD's opacity